Catalysis Science & Technology

PAPER

View Article Online
View Journal | View Issue

Cite this: *Catal. Sci. Technol.*, 2014, **4**, 2260

Received 10th February 2014,
Accepted 15th March 2014

DOI: 10.1039/c4cy00174e

www.rsc.org/catalysis

On the selective acid-catalysed dehydration of 1,2,6-hexanetriol†

Michael R. Nolan, Geng Sun and Brent H. Shanks*

Selectivity results for the dehydration of 1,2,6-hexanetriol over solid acid catalysts are reported. A slate of catalysts including zeolites, amorphous silica-alumina, and niobias were tested and the selectivity towards either cyclic ethers or α,ω-dioxygenates was found to be mildly correlated with the acid strength of the fresh catalyst. In general, a ring closing dehydration reaction to a pyran was the dominant reaction pathway. Differences in the catalysts were mitigated by significant coke formation.

Introduction

Biorenewable feedstocks for commodity chemicals are well recognized as potential alternatives to petroleum-based feedstocks,[1–3] but their high oxygen content requires selective oxygen removal in order to produce these chemicals. Deoxygenation strategies are driven by the type of carbon–oxygen bond that is found in the biorenewable molecule, with aldehydes and acids normally calling for carbon removal by decarbonylation or decarboxylation. In the case of polyhydroxylated molecules, however, it is possible to utilize dehydration to selectively remove oxygen while preserving carbon.

Previous work on selective dehydration of polyols has focused primarily on dehydration of glycerol and diols over acid catalysts.[4–9] In work by Sato *et al.* with glycerol, butanediols, and pentanediols, it was found that dehydration of a diol will lead selectively to formation of a cyclic ether if the second hydroxyl is positioned γ or farther relative to the hydroxyl being dehydrated.[9] Diols with β positioned hydroxyls tend to be more selective to allylic alcohols, and diols with α positioned hydroxyls tend to form an enol, and tautomerize to a ketone or aldehyde,[9] It was also found that at temperatures below 673 K, the dehydration reaction also tends to proceed until a mono-oxygenate was reached and then ceased.[10,11] The general dehydration rule found across these papers is that diol interactions and resulting products tend to be driven by the relative positions of the hydroxyl groups in the diols.

More recent work on the dehydration of polyols has focused on 1,2,6-hexanetriol (**1**, Scheme 1), which can be derived from HMF.[12] Work in this area has focused on selective removal of the 2-position hydroxyl in order to produce 1,6-hexanediol (1,6-HDO, **6** in Scheme 1), while avoiding formation of the byproduct tetrahydropyran-2*H*-2-methanol (THP-2-M, **2** in Scheme 1).[12,13] Results from the previous work have found that formation of THP-2-M is largely unavoidable in condensed-phase reaction conditions. Therefore the preferred route to α,ω-diols was to convert 1,2,6-hexanetriol quantitatively to THP-2-M, and selectively ring-open the pyran over acid-promoted hydrogenating metals.[13] The reaction conditions in this work was performed under high hydrogen pressure, high catalyst loadings, and low reaction rates. As such, these systems were optimized to operate at slow dehydration conditions and fast hydrogenating conditions, which limited the ability to observe intermediates in the

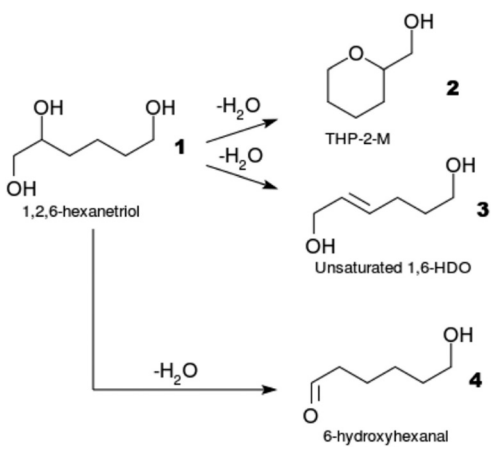

Scheme 1 Postulated reaction scheme for the dehydration of 1,2,6-hexanetriol.

1140L Biorenewables Research Laboratory, Ames, IA 50011, USA.
E-mail: bshanks.iastate.edu; Fax: +1 5152941269; Tel: +1 5152941895

† Electronic supplementary information (ESI) available. See DOI: 10.1039/c4cy00174e

dehydration pathway but did achieve selective conversion to 1,6-HDO. Chia *et al.* Found that hydrogenating metals on their own tended to select products based on minimizing steric hindrance and hydrogenating metals alloyed with oxophilic metals, which were also observed to have acidic tendencies, tended to ring-open at more substituted locations on a furan or pyran ring.[13]

In the previous work, the presence of catalytic acidity was noted as being critical to the dehydration reaction and to selective ring-opening of pyrans. However, the complete role of acidity in dehydration is still in question, along with the question of which acid catalyst properties can be manipulated to drive selectivity. In the current work, 1,2,6-hexanetriol was employed as a model compound to understand the catalytic drivers for selectivity in the dehydration of polyols. Acid strength and shape selectivity were investigated as variables in controlling activity and selectivity in the dehydration reaction, with selectivity defined primarily as selectivity to either linear α,ω-dioxygenates or to pyrans.

Methods

Catalyst slate

A slate of solid acid catalysts was chosen to test the effects of acid strength and shape selectivity. The slate included zeolites, H-ZSM5, Y-zeolite, and mordenite, niobia supported on silica (SBA-15) and amorphous metal oxides, silica–alumina and niobia. The silica–alumina ratios of the tested catalysts are given in Table 1. All of the zeolites were obtained from Zeolyst International, and were calcined in air at 773 K for 4 hours prior to use. The niobia catalysts were used as received with amorphous niobia catalyst being a commercial sample from CBMM and the niobia on SBA-15 synthesized according to the procedure from Pham *et al.*[14]

The silica–alumina catalyst was prepared by precipitation using the following method: 48.8 g of sodium metasilicate and 1.57 g of aluminum sulfate hexadecahydrate, in accordance with the desired silica–alumina ratio, were dissolved in 500 mL of water in a stirred round-bottom flask. Once the reagents were fully dissolved, hydrochloric acid (stock solution diluted to 10 vol% in deionized water) was added until the solution began to precipitate at a pH of about 8.5. The acid was then added dropwise until the solution reached a pH of approximately 7. The precipitate was then filtered in a vacuum filtering flask and washed 3 times with deionized water. The filter cake was dried at 383 K for 24 hours (until the gel was fully dried) and then crushed in a mortar and pestle to produce a catalyst powder. Finally, the powder was calcined in air at 773 K for 4 hours.

Prior to reaction testing, the catalysts were pelleted in a Carver benchtop pellet press at 2760 bar, broken into small pellets, and sieved to achieve a pellet size range from 700 μm to 1 mm.

Catalyst characterization

The catalysts were characterized using the Brunnauer–Emmet–Teller (BET) method for surface area and temperature programmed desorption (TPD) with ammonia for active site characterization. A typical BET experiment was performed as follows: 0.1 g of a catalyst sample was brought to a 10 μm Hg vacuum and heated to 423 K for 6 hours. Then, a nitrogen BET isotherm was recorded using a Micromeritics ASAP 2020 and the surface area and approximate pore size were determined.

A typical TPD experiment was performed in a Micromeritics AutoChem 2920 by heating approximately 60 mg of the catalyst sample in helium gas from ambient temperature to 923 K at a rate of 10 K min^{-1} in order to eliminate chemisorbed water as well as to determine the water desorption temperatures. The sample was then cooled to 323 K, exposed to a 90% helium/10% ammonia gas mixture for 30 minutes, and exposed to pure helium by switching the gas until any residual ammonia gas was purged from the sample container. The purged sample was heated to 923 K in helium using 10 K min^{-1} temperature ramp rate and the quantity of ammonia desorbed over the temperature range was determined.

After use, the catalysts were again characterized using ammonia temperature programmed desorption with the analysis combined with mass spectral analysis of the effluent gases. A typical experiment was performed by exposing approximately 40 mg of the catalyst sample to a 90% helium/10% ammonia gas mixture for 30 minutes. Then, the sample was heated in helium from ambient temperature to 723 K at a temperature ramp rate of 10 K min^{-1} while monitoring the effluent gases with a MicroStar mass spectrometer.

Flow reactor studies with 1,2,6-hexanetriol

Neat 1,2,6-hexanetriol was injected into a heated stainless steel preheating tube using syringe pump at a rate of 5 ml h^{-1}.

Table 1 Properties of catalyst slate

Catalyst	Si/Al ratio	TPD acid strength (peak temp., K)	Acid site density (mmol g^{-1})	Surface area (m^2 g^{-1})	Pore size Å
Niobia	n/a	506	0.28	140	40.9[a]
Niobia/SBA-15	n/a	484	0.20	113	46.5[a]
Silica–alumina	80 : 1	465	0.29	594	45.7[a]
H-ZSM5	30 : 1	657	0.48	571	5.5[b]
H-ZSM5	80 : 1	625	0.18	381	5.5[b]
Zeolite Y	80 : 1	544	0.06	676	7.4[b]
H-mordenite	90 : 1	642	0.33	469	6.5[b]

[a] Determined from BET data. [b] Literature values from Chen *et al.*[18]

Argon was also co-fed at a flow rate of 100 ml min^{-1} at STP. The triol evaporated and mixed with the argon inside the preheating tube and the resulting vapor stream was then flowed into a packed-bed flow reactor (12 mm OD steel tube, 15 cm long bed). The bed was packed with a measured quantity of catalyst diluted in 1 mm glass beads. Temperatures were monitored at the end of the preheating tube as well as the entrance and exit of the packed bed. All three temperatures were maintained within 2 K of the set point temperature. The effluent stream from the reactor passed into a condenser, where the products condensed on the inner walls and the condensate then dripped into a collection vial. The residence time of the condenser was held at 1 min, as shorter residence times led to insufficient condensation. The argon in the effluent stream exited the condenser through an exit line at the top of the condenser and the liquid products were collected in a vial at the bottom of the condenser.

The product samples were highly viscous and required a relatively long time to exit the condenser, so sample blending was minimized by operating the reactor continuously. In a given experiment, 5 product samples were taken for each catalyst with the samples prepared for analysis by diluting to 10 wt% in water (0.9000 grams water, 0.1000 grams sample) and adding 10 μL of methanol as an internal standard. Once prepared, the samples were analyzed in an Agilent 7890 gas chromatogram equipped with a flame ionization detector and mass spectrometer. Product molecules not readily identified, *i.e.*, those with less than 85% statistical match in the NIST mass spectral libraries, were interpreted manually and the interpretation is given in the ESI.†

All experiments were replicated at least once to measure experimental consistency. Only replicated experiments in which the overall mass balance was greater than 90% were included in the published results. The reason for mass loss was related to catalyst coking during the reaction (~1% loss) or to losses in the reagent inlet line (3–5% loss). Those discarded runes in which the mass balance was below 90% could be attributed to vapor losses in the condenser, which made the selectivity results unreliable due to losses of volatile compounds.

Deactivation of the catalysts due to coking was commonly observed during the study, with much of the deactivation occurring during the beginning of an experimental run. To account for this, data for the first sample (the deactivation sample) of a given experiment was treated separately from the remaining four samples (steady-state samples) in an experiment, which were averaged to give the reported values.

Each of the catalysts were tested according to the above flow reaction procedure at 573 K. The weight of catalyst added was based on a constant number of high-strength acid sites, which was determined by multiplying catalyst mass by acid site density (Table 1) to get the number of acid sites for that sample. 50 mg of H-ZSM5, 30/1 Si/Al ratio (0.024 mmol of high-strength acid sites) was used as the basis for determining the required mass loading for the other catalysts, as this catalyst had the highest acid site density amongst the catalysts tested.

10 wt% solutions of THP-2-M and 1,6-hexanediol in water were used as reagents following the same flow reactor procedure outlined above. The reactions were performed at 573 K, using the same molar flow of reagent as was used in the 1,2,6-hexanetriol runs. 133 mg of H-ZSM5 (80/1 Si/Al ratio) was used as the catalyst.

Results

Catalyst properties

The catalyst slate was selected to provide sufficient variance in terms of acid strength and pore size as to examine the importance of these factors. The measured properties of the catalysts are given in Table 1. The acid strengths for the fresh catalysts, as measured by ammonia TPD, spanned the typical range that has been commonly reported in the literature.[15–17] Per previous reports, weak acid sites were attributed to the temperature range from 423 to 523 K, and the strong acid sites to peaks ranging from 573 to 773 K. In terms of shape selectivity, the average pore diameters for the zeolites and non-zeolites varied by an order of magnitude.

Reaction testing

Catalyst activity was measured by quantifying the amount of 1,2,6-hexanetriol that was consumed and appeared as GC-identifiable products. Losses attributed to deposition of the triol in transfer lines were excluded from the overall reaction rate. GC analysis of the non-condensable gases found that cracking of the triol to smaller molecules was negligible and losses due to catalyst coking accounted for less than 1% of the reaction products.

The turnover frequency of each catalyst is reported in Fig. 1 as a function of TPD peak temperature. All of the catalysts deactivated significantly from the start of the experiment until a relatively stable operation was achieved. The decrease in activity was as much as an order of magnitude. Overall, the acid strength and activity were only weakly correlated after the first sample point (still in the deactivation region) and the correlation remained weak for the remaining samples. TPD analysis of the used catalysts showed that both the strong and weak acid sites were significantly diminished and in most cases the strong acid sites appeared to have been completely suppressed for the catalysts. As an example, the

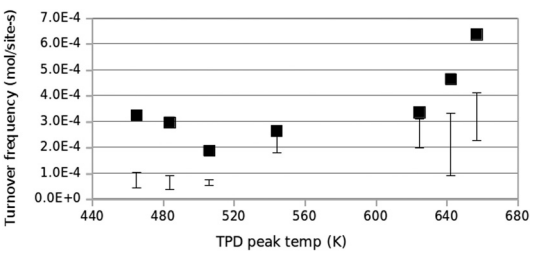

Fig. 1 Activity of acid catalysts, as measured by turnover (moles converted per acid site per second). Activity was measured both for the first sample taken (■), and for the four following samples (bars). The bars denote the complete range of observed activities.

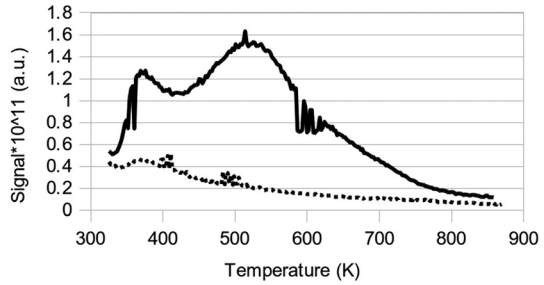

Fig. 2 Ammonia TPD profile of fresh (solid line) and spent (dashed line) amorphous niobia catalyst. The stronger site at ~520 K appears to be completely suppressed by the end of the reaction.

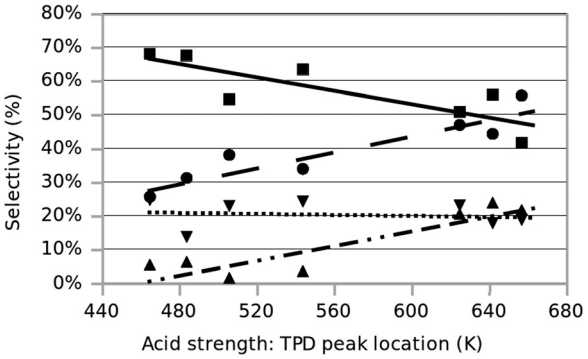

Fig. 3 Selectivity to pyrans and major pyran compounds as a function of acid strength. Products shown include mono pyrans (■, solid line), all linear and linear-origin compounds (●, dashed line), linear 1,6 dioxygenates (▼, dotted line), and condensed linear products (▲, dot-dash line).

acid site suppression for the used amorphous niobia is shown in Fig. 2 in which essentially all of the strong acid sites observed for the fresh catalyst were found to disappear for the used catalyst. TPD profiles for the other used catalysts are given in the ESI.†

As measured by TGA, catalyst coking was also observed on all of the used catalysts, with coking accounting for about 14% of the mass of the used catalyst on average. Based on this observation and the TPD results, coking was the probable cause for both the loss of active sites and the apparent corresponding loss in specific activity.

The majority (>95%) of the six-carbon molecule products observed during the dehydration reaction are shown in Scheme 2 and could be classified as being either "linear" (3, 4, 5, 6) or "pyran" (2, 7, 8). Condensation products are not shown in Scheme 2, but based on MS analysis (see ESI† A), the products most likely originated from condensation of the aldehyde products.

Selectivity as a function of acid strength as defined by TPD peak position for the fresh catalyst is given in Fig. 3. The selectivity values were averaged over the four final samples in each run. The pyran ring products decreased from 68 to 42 mol% with increasing acid strength values (Table 2).

Among the linear products, the selectivity to mono-oxygenated products (hexenals and hexenols) increased with acid strength. This increase was particularly pronounced when the TPD peak acid strength was above 623 K. Another interesting phenomenon observed over the catalysts was hydride transfer between molecules with 1,6-HDO being the sole observed hydrogenation product. The selectivity to 1,6-HDO was found to be up to 11 mol% over the weak acid catalysts, but this selectivity to the saturated diol decreased with increasing acid strength. Selectivity to dehydrogenated products such as 7 and 8 from Scheme 2 typically comprised 6–8 mol% of the total product selectivity and had no correlation with acid strength.

1,2- and 1,5-dioxygenates were not observed in any significant quantity over any catalyst, which strongly implied that the heterogeneous acid catalysts used in this study were highly selective toward removing the secondary hydroxyl. It appeared that dehydration of the primary hydroxyls only occurred in the case of a further dehydration of generated

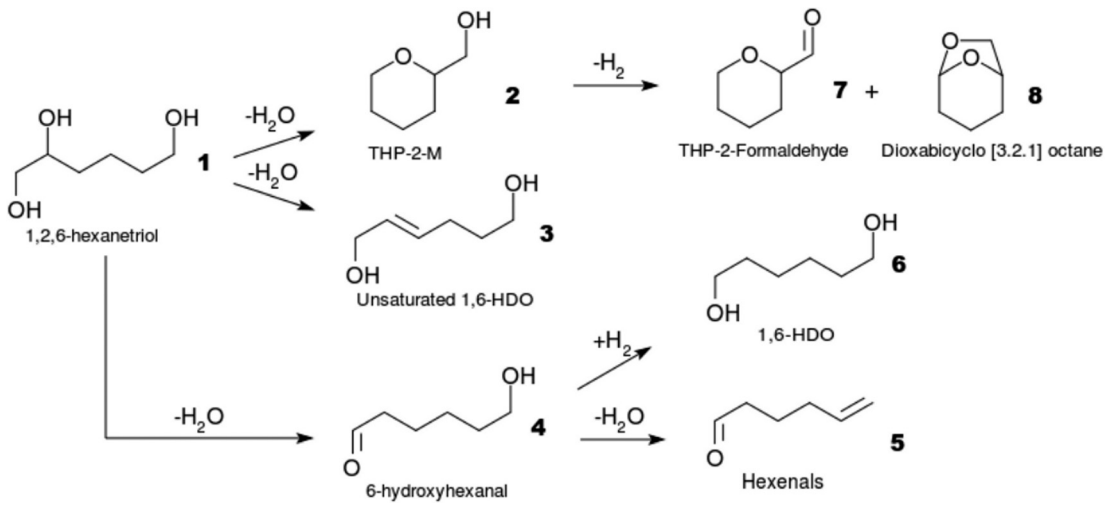

Scheme 2 Reaction scheme for the dehydration of 1,2,6-hexanetriol, based on product observations.

Table 2 Selectivities of tested catalysts (mol%)

Catalyst	Si/Al ratio	Mass balance	Conversion	Saturated 1,6-diol	1,6 Diol and precursors	All pyrans	All linear	Others
Niobia	n/a	98%	3%	11%	23%	54%	38%	7.57%
Silica–niobia	n/a	93%	2%	3%	14%	67%	31%	1.45%
Silica–alumina	80 : 1	95%	10%	0%	25%	68%	26%	6.55%
H-ZSM5	30 : 1	95%	13%	2%	19%	42%	56%	2.92%
H-ZSM5	80 : 1	95%	9%	2%	23%	51%	47%	2.48%
Zeolite Y	80 : 1	91%	6%	5%	24%	63%	34%	2.86%
H-mordenite	90 : 1	95%	11%	0%	18%	56%	44%	0.00%

dioxygenates to mono-oxygenates. This observation was again consistent with a Brønsted-catalyzed elimination, as the cation that would result from the elimination of the secondary hydroxyl group would be more stable than those arising from the elimination of a primary hydroxyl.

Selectivity to monofunctional pyrans, condensation products, and mono-oxygenates were found to be correlated with zeolite pore size, with the trends shown in Fig. 4. Overall, smaller pores tended to lead to fewer mono-pyrans and to more condensation products and mono-oxygenates. At the large pore end as seen in Fig. 4, selectivity to condensation products became consistent with that of the amorphous materials in the catalyst slate, indicating that pores are "large" by the time they reach the micropore size of zeolite Y (~7.4 Å). The enhanced selectivity toward condensation products indicated that smaller pores did not lead to enhanced selectivity toward linear dioxygenates, but instead promoted reactions between molecules, which would be an undesired effect for selective dehydration.

Reactions studies performed with THP-2-M over H-ZSM5 (80 : 1 Si : Al ratio) yielded only a small quantity of condensation products (~2% yield), and a small amount of THP-2-formaldehyde (~1% yield). No ring-opening was observed when THP-2-M was fed to the reactor, indicating that ring opening did not play a role in the formation of linear products and that a ring-opening reaction pathway for forming 1,6-HDO from 1,2,6-hexanetriol would not occur over an acid catalyst. The formation of THP-2-formaldehyde was indicative of the ability of acid catalysts to strip hydrogen from primary alcohols, which would contribute toward selectivity to dehydrogenated products such as THP-2-formaldehyde and dioxabicyclo [3.2.1] octane.

Reactions with 1,6-hexanediol and H-ZSM5 (80 : 1 Si : Al ratio) as the catalyst yielded only a small amount (~1% yield) of hexenols. The low reactivity of either 1,6-hexanediol or THP-2-M were indicative of dioxygenates being significantly less reactive than 1,2,6-hexanetriol, which highlighted a trend of polyols becoming less active for dehydration as more oxygen is removed.

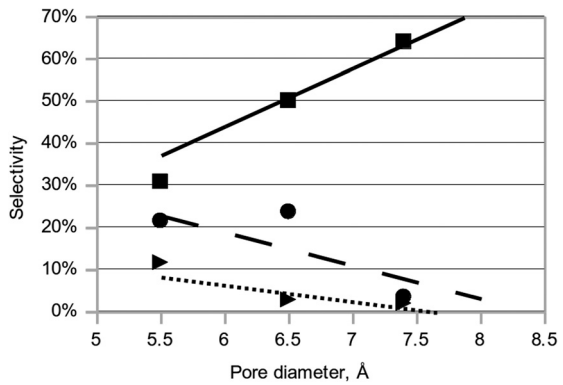

Fig. 4 Selectivity *versus* pore diameter for the zeolite catalysts with pore diameters taken from literature values.[19] Products found to vary with zeolite pore diameter included mono-pyrans (■, solid line), condensation products (●, dashed line), and mono-oxygenates (▼, dotted line).

Discussion

Reaction scheme

Dehydration is generally understood to be a Brønsted acid-catalyzed reaction,[20] and selectivity to both pyrans and 1,6-dioxygenates along with terminal mono-oxygenates in this study was consistent with that conclusion. The absence of either ring-opening or ring-closing from THP-2-M or 1,6-hexanediol indicated that ring opening as observed in other work[13] required the presence of a metal functionality. This observation led to the proposed reaction pathway given in Scheme 2, in which ring and linear selectivity was determined when 1,2,6-hexanetriol first dehydrated and after that all of the derivative products emerged from these primary products of triol dehydration. Previous work on dehydration has postulated likely cationic intermediates for Brønsted acid-catalyzed dehydration,[13] which are shown in Fig. 5 as a proposed reaction pathway.

In addition to products expected directly from acid-catalyzed dehydration, products that were hydrogenated or

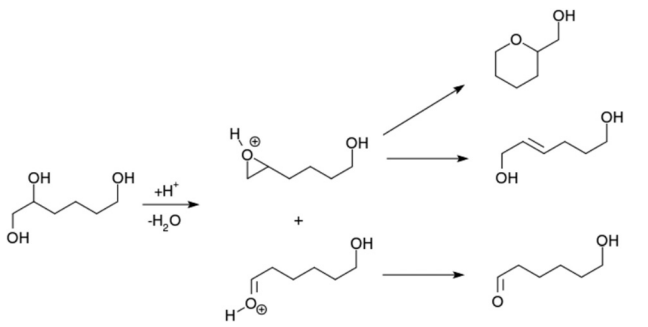

Fig. 5 Proposed reaction map for acid-catalyzed dehydration of 1,2,6-hexanetriol.

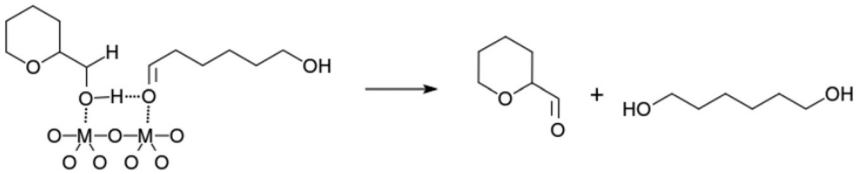

Fig. 6 Illustration of the MPV reaction over a metal oxide.

dehydrogenated relative to these expected products were also present, as were compounds that appeared to emerge from the juncture of two or more C6 molecules. These products were all proposed to originate from 6-hydroxyhexanal, which was produced during the dehydration step. It is well developed in the literature that alcohols and aldehydes readily undergo hydride transfer over metal oxides, with aluminium oxide being a particularly good metal oxide for the reaction. This reaction, known as the MPV reduction reaction (see Fig. 6), would account for the hydrogenation of 6-hydroxyhexanal to 1,6-hexandiol as observed over select catalysts, along with the dehydrogenation of THP-2-M and other molecules to aldehydes.

Role of catalyst properties

The role of acid strength in dehydration activity was found to be difficult to elucidate from reaction testing as catalyst deactivation *via* coking was occurring in concert with the dehydration reaction. This coking was found to lead to a reduction of the number of available sites. Relative to catalyst selectivity, increasing the catalyst acid strength led to a modest increase in selectivity towards linear products. However, instead of producing more precursors to 1,6-hexanediol, the linear products were instead observed to condense more readily with these more acidic catalysts, leading to a flat selectivity toward 1,6-dioxygenates over the entire range of acid strengths. It was also observed that MPV-type hydride transfers tended to be favored over weaker acids, whereas stronger acids favored dehydrogenating alcohols without transferring the hydrogen to aldehydes. Size selection was also found to play a role in selectivity as smaller pores led to decreased selectivity to pyrans, and increased selectivity to condensation products.

In the context of creating catalyst design rules for the selective dehydration to polyols, the major barrier identified for solid acids was an apparent ceiling in their selectivity towards α,ω-dioxygenates. Weak acid catalysts tended to be selective toward ring formation, while stronger acids tended to promote condensation of 6-hydroxyhexanal. The hydroxyaldehyde also participated in a second pathway in the reaction scheme as it could participate in a MPV-type hydride transfer, which led to the formation of alcohols and aldehydes that would not be expected from acid-catalyzed dehydration alone. Forming hydroxyaldehydes from polyols may open up interesting new avenues if one were to optimize a system for carrying out subsequent hydride transfers, but in the case of selective dehydration to produce diols, it would be desirable to prevent the further reaction of hydroxyaldehydes so as to prevent unwanted condensation or hydride transfer reactions.

Conclusions

The slate of acid catalysts tested represented a range of acid strengths and pore sizes, and general design rules were proposed based on acid strength and pore size effects. Dehydration of 1,2,6-hexanetriol over strictly acid catalysts readily ring-closed to pyrans, which did not subsequently ring open. Therefore, the efficient production of α,ω-diols and deoxygenates would require an alternative approach. The acid strength of the fresh catalyst was found to influence activity, but was mitigated by the significant loss of activity sites due to coking. A modest shift in selectivity was found to correlate with acid strength. Pore diameters, when sufficiently small, were found to play a role in aiding the condensation of dehydration products, which would be an undesirable effect.

Also of significant interest in understanding these acid catalysts was the observation of hydride transfer reactions occurring in what was expected to be a reaction environment that would only cause dehydration. Acid strength drove selectivity in hydride transfer, as higher acid strengths inhibited the MPV reduction of 6-hydroxyhexanal to 1,6-hexanediol.

Acknowledgements

We would like to acknowledge the support for this project from the Nation Science Foundation under the award EEC-0813570. We would also like to acknowledge the contribution of niobia catalysts from the Datye group from the University of New Mexico, which were used in the catalyst studies.

References

1 B. J. Nikolau, M. A. D. N. Perera, L. Brachova and B. Shanks, *Plant J.*, 2008, **54**, 536–545.
2 L. R. Jarboe, X. Zhang, X. Wang, J. C. Moore, K. T. Shanmugam and L. O. Ingram, *J. Biomed. Biotechnol.*, 2010, **2010**, 1–18.
3 C. Zhou, J. N. Beltramini, Y. Fana and G. Q. Lu, *Chem. Soc. Rev.*, 2008, **37**, 527–549.
4 H. Gotoh, Y. Yamada and S. Sato, *Appl. Catal., A*, 2010, **377**, 92–98.
5 V. Lehr, M. Sarlea, L. Ott and H. Vogel, *Catal. Today*, 2007, **121**, 121–129.
6 A. Igarashi, S. Sato, R. Takahashi, T. Sodesawa and M. Kobune, *Catal. Commun.*, 2007, **8**, 807–810.

7 S. Sato, R. Takahashi, T. Sodesawa, N. Honda and H. Shimizu, *Catal. Commun.*, 2003, **4**, 77–81.
8 E. Tsukuda, S. Sato, R. Takahashi and T. Sodesawa, *Catal. Commun.*, 2007, **8**, 1349–1353.
9 S. Sato, R. Takahashi, T. Sodesawa and N. Honda, *J. Mol. Catal. A: Chem.*, 2004, **221**, 177–183.
10 S. Sato, R. Takahashi, T. Sodesawa, A. Igarashi and H. Inoue, *Appl. Catal., A*, 2007, **328**, 109–116.
11 S. Sato, R. Takahashi, T. Sodesawa and N. Yamamoto, *Catal. Commun.*, 2004, **5**, 397–400.
12 T. Buntara, S. Noel, P. H. Phua, I. M. Cabrera, J. G. Vries and H. J. Heeres, *Angew. Chem., Int. Ed.*, 2011, **50**, 7083–7087.
13 M. Chia, Y. J. Pagan-Torres, D. Hibbitts, Q. Tan, H. N. Pham, A. K. Datye, M. Neurock, R. J. Davis and J. A. Dumesic, *J. Am. Chem. Soc.*, 2011, **133**, 12675–12689.
14 H. N. Pham, Y. J. Pagan-Torres, J. C. Serrano-Ruiz, D. Wang, J. A. Dumesic and A. K. Datye, *Appl. Catal., A*, 2011, **397**, 153–162.
15 K. Suzuki, Y. Aoyagi, N. Katada, M. Choi, R. Ryoo and M. Niwa, *Catal. Today*, 2008, **132**, 38–45.
16 K. Wang, X. Wang and G. Li, *Microporous Mesoporous Mater.*, 2006, **94**, 325–329.
17 R. Weingarten, G. A. Tompsett, W. C. Conner and G. W. Huber, *J. Catal.*, 2011, **279**, 174–182.
18 N. Y. Chen, T. F. Degnan and C. M. Smith, *Molecular Transport and Reaction in Zeolites: Design and Application of Shape Selective Catalysis*, Wiley–VCH, Weinheim, 1994.
19 L. Cheng and X. P. Ye, *Catal. Lett.*, 2009, **130**, 100–107.
20 J. Macht, R. T. Carr and E. Iglesia, *J. Catal.*, 2009, **264**, 54–66.

